Materials Science and Engineering, Volume 44, No. 2 (2019), pp. 43–53.
DOI: 10.32974.mse.2019.005

EFFECTS OF SPIN-ORBIT INTERACTION ON SURFACES AND INTERFACES

NÓRA KUCSKA[1]–ZSOLT GULÁCSI[2]

Itinerant 2D two-band systems as surfaces or interfaces are analysed in exact terms in the presence of on-site Coulomb repulsion in the correlated band, and many-body spin-orbit interactions present in both bands. The results show a strong dependence of the particle mobility on the spin-orbit interaction strengths, and also underline that in the high concentration limit, accentuated spin-projection dependence appears in the carrier mobility, which emphasize real application possibilities in spintronics. The spin-projection dependence of the mobility is motivated by the emergence of spontaneous magnetization on the surface, in the presence of spin-orbit interaction, which provide an explication why magnetic properties can appear at the interface of two non-magnetic materials.

Keywords: exact solutions, spin-orbit coupling, strongly correlated systems

INTRODUCTION

Surfaces and interfaces are basic components of main electronic devices controlling and processing the electronic and digital equipment present on a broad spectrum of modern technologies. Indeed, the functionality of semiconducting components, semiconducting and metallic multilayers and interlayers is governed by specially constructed, treated, deposited, configured or formed surfaces and interfaces. On these two dimensional entities, especially in a direction perpendicular to them, potential gradients always appear, which via the Dirac equation introduce the many-body spin-orbit interactions [1] in all processes in which conducting or itinerant carriers play a main role even at non-relativistic level [2]. Often used specific components of this interaction are known as Rashba [3], or Dresselhaus [4] couplings. Written at second quantized level, these provide specific spin-flip type of hopping terms in the one-particle part of the Hamiltonian [5].

Often it happens that many-body processes that take place on surfaces are strongly correlated because usually, given especially by the logarithmic shape of the Coulomb potential in 2D [6], the inter-electronic interactions are strong on surfaces, as in the case of e.g. GaAs heterostructures [7], iridium based heterostructures or iridates [8], perovskites [9], heterostructures with organic materials [10], etc. Contrary to this, the

[1] Department of Theoretical Physics, University of Debrecen
4026 Debrecen, Bem tér 18/a., Hungary
e-mail address: kucska@phys.unideb.hu
[2] Department of Theoretical Physics, University of Debrecen
4026 Debrecen, Bem tér 18/a., Hungary
e-mail address: gulacsi@phys.unideb.hu

spin-orbit many-body coupling strength is small, often 4 order of magnitudes smaller than the highest representative of the Coulomb coupling, namely the on-site repulsion.

But even in this case, the spin-orbit interaction produces essential effects, since being arbitrary small, breaks the spin-projection double degeneracy of each band. As a consequence in this case perturbative treatment, being inconclusive, cannot be applied [11], and consequently the interplay of inter-electronic interactions and spin-orbit coupling is less explored [12], hence is not understood in details [8].

The aim of this paper is to partially fill up this gap. In order to deduce valuable results in conditions in which perturbative treatment cannot be applied, we use exact methods. Since the studied 2D systems are non-integrable, the applied technique is special, and will be presented below.

1. THE USED TECHNIQUE

The used method transforms in the first step in exact terms the system Hamiltonian in positive semidefinite form

$$\hat{H} = \hat{O} + C, \tag{1}$$

where $\hat{O}$ is a positive semidefinite operator, while C is a constant.
Usually, $\hat{O} = \sum_n \hat{O}_n$ is obtained as a sum over positive semidefinite operators $\hat{O}_n$. For a fixed $n = n_1$, the $\hat{O}_{n_1}$ expression can be given e.g. by a construction based on block operators $\hat{A}_{i_{n_1}}$ as $\hat{O}_{n_1} = \hat{A}_{i_{n_1}}^{\dagger}\hat{A}_{i_{n_1}}$, or by special expressions as e.g. at $n = n_2$, $\hat{O}_{n_2} = \hat{P}_{n_2} = \hat{n}_{i_{n_1},\uparrow}\hat{n}_{i_{n_1},\downarrow} - (\hat{n}_{i_{n_1},\uparrow}\widehat{+n}_{i_{n_1},\downarrow}) + 1$.The block operators $\hat{A}_i = \sum_{i,\sigma} p_{j,\sigma}\hat{c}_{j,\sigma}$ are linear combinations of Fermi annihilation operators $\hat{c}_{j,\sigma}$ acting on the sites $j \in B_i$ of a finite block B_i, connected to the site i. The numerical refactors $p_{j,\sigma}$ are block operator parameters.

In order to transform the Hamiltonian in the positive semidefinite form (1), the connected Matching system of equations must be solved. This is obtained because the left side of (1) depends on the Hamiltonian parameters (hopping matrix elements, on-site one-particle potentials, hybridization strengths, etc.), while the right side of (1) is dependent on the block operator parameters and the constant C. Consequently, in order to have the exact identity (1) satisfied, relationships must be present in between the Hamiltonian parameters, the block operator parameters and C.

These equalities build up the Matching system of equations. These equations are usually coupled, non-linear and complex-algebraic equations. Solving them one obtains the explicit expression of the block operator parameters and the constant C.

Once the transformation in positive semidefinite form (1) has been performed, in the second step of the method one deduces the exact multielectronic ground state $|\psi_G\rangle$. Since the minimum possible eigenvalue of a positive semidefinite operator is zero, the exact ground state is provided by the most general solution $|\psi_G\rangle$, of the equation $\hat{O}|\psi_G\rangle = 0$. If necessary, the uniqueness of the solution can also be proved on the line of [13]. The parameter space region in which the deduced ground state is

valid is provided by the parameter domain in which the obtained solution of the Matching system of equations is valid. The ground state energy corresponding to $|\psi_G\rangle$ is provided by the relation $E_G = C$.

In the third step of the method, using the obtained $|\psi_G\rangle$, one calculates the physical properties of the deduced phase by calculating ground state expectation values of different physical quantities of interest.

Also exact results relating the low laying part of the excitation spectrum are possible to be obtained, see [13].

The here presented procedure can be applied always independently on dimensionality and integrability. The technical steps necessary to be used in the presented first two steps have been worked out in extreme details [13–16], and the procedure has been successfully applied before in several many-body cases of large interest, including three dimensions [17], two dimensional disordered systems [18], or stripes, checkerboards and droplets in 2D [19]. The novelty in using the method in the present case is that in transforming the Hamiltonian in positive semidefinite form, two block operators are used containing the components of both spin projections of fermionic carriers.

The remaining part of the paper is structured as follows: Sect. II presents the studied system, Sect. III describes the obtained results, Sect. IV. concludes the paper, and the Appendix containing the mathematical details closes the presentation.

2. THE STUDIED SYSTEM

One analyses a realistic itinerant surface or interface which is always of multiband type. For multiband materials the theoretical description is given usually by projecting the multiband structure in a few-band picture present around the Fermi surface [20], projection which is stopped here for its workability, at two-band level. One of these bands (denoted conventionally by f) is considered correlated, while the second band (denoted formally by d) is taken into account in a non-correlated form. In between these bands, as in real materials, hybridization is present whose strength is denoted by V.

Also for its simplicity, one considers here a 2D orthorhombic Bravais lattice present on the surface. Concerning the inter-electronic interaction, given by the strong screening present in itinerant many-body systems, one takes into account the main component of the Coulomb interaction in such cases, namely the on-site Coulomb repulsion U_f present in the correlated band. The hopping matrix elements are denoted by t, while the on-site one-particle potentials by ε. The Hamiltonian of the system is given by $\hat{H} = \hat{H}_{kin} + \hat{H}_{int} + \hat{H}_{SO}$, where

$$\hat{H}_{c,0} = \sum_i \sum_{\alpha=\uparrow,\downarrow} \varepsilon_c \, \hat{c}_{i,\alpha}{}^{\dagger} \hat{c}_{i,\alpha}, \quad \hat{V}_0 = \sum_i \left[\left(\sum_{\alpha=\uparrow,\downarrow} V_0^{d,f} \hat{d}_{i,\alpha}{}^{\dagger} \hat{f}_{i,\alpha} \right) + H.c. \right],$$

$$\hat{H}_{c,p} = \sum_i \left[\left(\sum_{\alpha=\uparrow,\downarrow} t_p^c \hat{c}_{i+p,\alpha}{}^\dagger \hat{c}_{i,\alpha} \right) + H.c. \right],$$

$$\hat{V}_p = \sum_i \left[\left(\sum_{\alpha=\uparrow,\downarrow} V_p^{d,f} \hat{d}_{i+p,\alpha}{}^\dagger \hat{f}_{i,\alpha} + V_p^{f,d} \hat{f}_{i+p,\alpha}{}^\dagger \hat{d}_{i,\alpha} \right) + H.c. \right],$$

$$\hat{H}_{kin} = \hat{V}_0 + \sum_{c=d,f} \hat{H}_{c,0} + \sum_{p=x,y} \left[\hat{V}_p + \sum_{c=d,f} \hat{H}_{c,p} \right], \quad \hat{H}_{int} = \sum_i U_f \hat{n}_{i,\uparrow}{}^f \hat{n}_{i,\downarrow}{}^f,$$

$$\hat{H}_{SO} = \sum_{c=d,f} \sum_i \left[\sum_{p=x,y} (t_{\uparrow,\downarrow}^{c,p} \hat{c}_{i+p,\uparrow}{}^\dagger \hat{c}_{i,\downarrow} + t_{\downarrow,\uparrow}^{c,p} \hat{c}_{i+p,\downarrow}{}^\dagger \hat{c}_{i,\uparrow}) + H.c. \right], \tag{2}$$

where $p = x, y$ are the Bravais vectors of the system, $\hat{n}_{i,\alpha}{}^f = \hat{f}_{i,\alpha}{}^\dagger \hat{f}_{i,\alpha}$, . Note that the spin-orbit coupling enters in $\hat{H}_{SO,c}$, where $c = d, f, \quad p = x, y$ and one has $t_{\uparrow,\downarrow}^{c,x} = t_R^c - it_D^c, \quad t_{\downarrow,\uparrow}^{c,x} = -t_R^c - it_D^c, t_{\uparrow,\downarrow}^{c,y} = t_D^c - it_R^c, \; t_{\downarrow,\uparrow}^{c,y} = -t_D^c - it_R^c$, where represents $t_R^c, (t_D^c)$ the Rashba (Dresselhaus) interaction strength.

3. THE OBTAINED RESULTS

For the transformation into positive semidefinite form two block operators have been used defined on the unit cell connected to the lattice site i.

$$\hat{A}_i = \sum_{c=d,f} \sum_{\alpha=\uparrow,\downarrow} (a_{c,1,\alpha} \hat{c}_{i,\alpha} + a_{c,2,\alpha} \hat{c}_{i+x,\alpha} + a_{c,3,\alpha} \hat{c}_{i+x+y,\alpha} + a_{c,4,\alpha} \hat{c}_{i+y,\alpha}),$$
$$\hat{B}_i = \sum_{c=d,f} \sum_{\alpha=\uparrow,\downarrow} (b_{c,1,\alpha} \hat{c}_{i,\alpha} + b_{c,2,\alpha} \hat{c}_{i+x,\alpha} + b_{c,3,\alpha} \hat{c}_{i+x+y,\alpha} + b_{c,4,\alpha} \hat{c}_{i+y,\alpha}). \tag{3}$$

The Hamiltonian transformed into a positive semidefinite form as mentioned above has the expression $\hat{H} = \hat{O} + C$, where $\hat{O} = \hat{O}_1 + \hat{O}_2$.

$$\hat{O}_2 = \sum_i (\hat{A}_i \hat{A}_i{}^\dagger + \hat{B}_i \hat{B}_i{}^\dagger), \quad \hat{O}_1 = U_f \sum_i \hat{P}_{i,}$$
$$C = \eta N - U_f N_{sit} - \sum_i \left(z_i^A + z_i^B \right), z_i^A = \left\{ \hat{A}_i, \hat{A}_i{}^\dagger \right\}, z_i^B = \left\{ \hat{B}_i, \hat{B}_i{}^\dagger \right\}, \tag{4}$$

where N represents the number of electrons, N_{sit} gives the number of lattice sites. After solving the connected Matching system of equations one obtains the explicit expression of the block operator parameters and η presented in the Appendix.

The exact ground state corresponding to the positive semidefinite form of the Hamiltonian has the expression

$$|\psi_G(N = N^*)\rangle = \prod_i [\hat{A}_i{}^\dagger \hat{B}_i{}^\dagger (\hat{f}_{i,\uparrow}{}^\dagger + \hat{f}_{i,\downarrow}{}^\dagger)]|0\rangle \tag{5}$$

where $|0\rangle$ represents the bare vacuum with no fermions present, and the product over i extends over all lattice sites. The presented ground state corresponds to the electron number $N = N^*$, where N^* is three times the number of lattice sites in the system ($N^* = 3N_{sit}$). For $N = N_1 + N^*$ the right side of (1) has to extend with a new operator, and a similar expression exists also for the case $N < \frac{N^*}{3}$.

Based on the obtained ground state wave function we deduced the long-range hopping ground state expectation value of $\hat{\Gamma}_{r,c,\sigma} = \frac{1}{N_{sit}} \sum_j (\hat{c}_{j,\sigma}{}^\dagger \hat{c}_{j+r,\sigma} + H.c.)$. This quantity was calculated for $c = d$ and in x direction, as can be seen in *Figure 1*. It shows a strong spin projection and spin-orbit coupling strength dependence. This remains true for arbitrary direction, and is motivated by the nonzero value of the ground state expectation value of the total spin $\hat{S}_z$ operator, signaling the emergence of spontaneous magnetization on the surface in the presence of spin-orbit coupling in the studied case. Since the long-range hopping determines the mobility of particles, the enumerated properties remain true also for the carrier mobility.

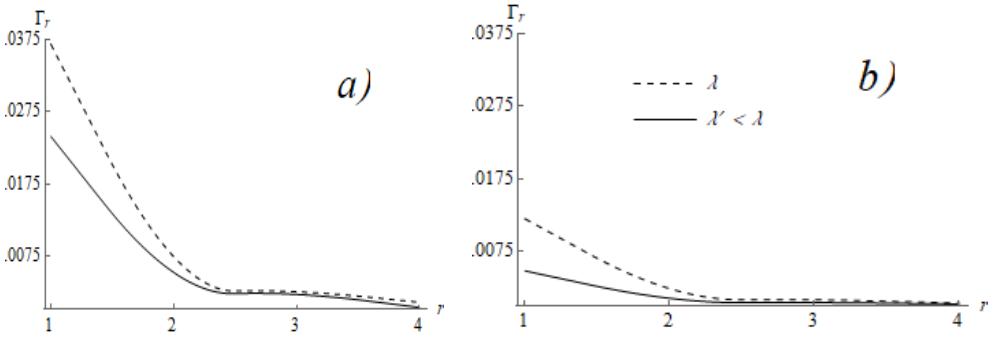

Figure 1

The r dependent hopping ground state expectation value Γ_r in function of the effective spin-orbit interaction $\lambda = \frac{1}{2}\sum_{c=d,f}\sqrt{(t_D^c)^2 + (t_R^c)^2}$ exemplified for d electrons in x direction. The distance r is given in lattice constant units. In the plot one has in t_x^f units $\lambda = 0.0603$, and $\lambda' = 0.0307$ respectively. Note that if λ increases, Γ_r increases as well and one has a strong spin projection dependence. The presented cases: a) negative spin projection to the Z axis, b) positive spin projection to the Z axis.

CONCLUSION

Realistic itinerant surfaces with inter-electronic on-site Coulomb repulsion and many-body spin-orbit interactions have been described in exact terms using a technique based on positive semidefinite operator properties. The method can always be applied for many-body systems independent on dimensionality and integrability. The Hamiltonian containing only local and nearest-neighbour terms has been transformed in positive semidefinite form, the exact ground state has been deduced, and ground state properties analysed. In the high concentration limit a strong dependence of the carrier mobility on spin projection and the strength of the spin-orbit interaction has been observed together with the emergence of ferromagnetism on the surface.

ACKNOWLEDGEMENT

Z. G. acknowledges the support of the project NKFI-128018 of Hungarian funds for basic research, and of the Alexander von Humboldt Foundation.

APPENDIX

This appendix presents the explicitly deduced block operator parameters.

$$b_{1,f,\uparrow} = \sqrt{\frac{(|v|-1)^2}{2\sqrt{2}(|v|+1)^2}\frac{|v|}{|u|}}\sqrt{\Theta_\uparrow}e^{i(\gamma+\phi_u+\delta_\uparrow)/2},$$

$$b_{1,f,\downarrow} = \sqrt{\frac{(|v|-1)^2}{2\sqrt{2}(|v|+1)^2}\frac{|v|}{|u|}}\sqrt{\Theta_\downarrow}e^{i(-\gamma+\phi_u+\delta_\downarrow)/2},$$

$$b_{2,f,\uparrow} = \frac{v\sqrt{2}}{|(|v|-1)|}\sqrt{\frac{(|v|-1)^2}{2\sqrt{2}(|v|+1)^2}\frac{|v|}{|u|}}\sqrt{\Theta_\downarrow}e^{i(\phi_u+\delta_\downarrow)/2},$$

$$b_{2,f,\downarrow} = \frac{v\sqrt{2}}{|(|v|-1)|}\sqrt{\frac{(|v|-1)^2}{2\sqrt{2}(|v|+1)^2}\frac{|v|}{|u|}}\sqrt{\Theta_\uparrow}e^{i(\phi_u+\delta_\uparrow)/2},$$

$$b_{3,f,\uparrow} = -\frac{1}{x^*}\sqrt{\frac{(|v|-1)^2}{2\sqrt{2}(|v|+1)^2}\frac{|v|}{|u|}}\sqrt{\Theta_\uparrow}e^{i\frac{(\gamma+\phi_u+\delta_\uparrow+2\phi)}{2}},$$

$$b_{3,f,\downarrow} = \frac{1}{x^*}\sqrt{\frac{(|v|-1)^2}{2\sqrt{2}(|v|+1)^2}\frac{|v|}{|u|}}\sqrt{\Theta_\downarrow}e^{i\frac{(-\gamma+\phi_u+\delta_\downarrow+2\phi)}{2}},$$

$$b_{4,f,\uparrow} = -\frac{1}{v^*}\frac{v\sqrt{2}}{|(|v|-1)|}\sqrt{\frac{(|v|-1)^2}{2\sqrt{2}(|v|+1)^2}\frac{|v|}{|u|}}\sqrt{\Theta_\uparrow}e^{i\frac{(\phi_u+\delta_\uparrow+2\phi)}{2}},$$

$$b_{4,f,\downarrow} = \frac{1}{v^*}\frac{v\sqrt{2}}{||v|-1|}\sqrt{\frac{(|v|-1)^2}{2\sqrt{2}(|v|+1)^2}\frac{|v|}{|u|}}\sqrt{\Theta_\downarrow}e^{i\frac{(\phi_u+\delta_\downarrow+2\phi)}{2}},$$

$$b_{1,d,\uparrow} = \frac{u_\uparrow}{v}\sqrt{\frac{(|v|-1)^2}{2\sqrt{2}(|v|+1)^2}\frac{|v|}{|u|}}\sqrt{\Theta_\downarrow}e^{-i\frac{(-\gamma+\phi_u+\delta_\downarrow+2\phi)}{2}},$$

$$b_{1,d,\downarrow} = -\frac{u_\downarrow}{v}\sqrt{\frac{(|v|-1)^2}{2\sqrt{2}(|v|+1)^2}\frac{|v|}{|u|}}\sqrt{\Theta_\uparrow}e^{-i\frac{(\gamma+\phi_u+\delta_\uparrow+2\phi)}{2}},$$

$$b_{2,d,\uparrow} = \frac{u_\uparrow}{v}\frac{v^*\sqrt{2}}{||v|-1|}\sqrt{\frac{(|v|-1)^2}{2\sqrt{2}(|v|+1)^2}\frac{|v|}{|u|}}\sqrt{\Theta_\downarrow}e^{-i\frac{(\phi_u+\delta_\downarrow+2\phi)}{2}},$$

$$b_{2,d,\downarrow} = -\frac{u_\downarrow}{v}\frac{v^*\sqrt{2}}{|(|v|-1)|}\sqrt{\frac{(|v|-1)^2}{2\sqrt{2}(|v|+1)^2}\frac{|v|}{|u|}}\sqrt{\Theta_\uparrow}e^{-i\frac{(\phi_u+\delta_\uparrow+2\phi)}{2}},$$

$$b_{3,d,\uparrow} = -\frac{u_\uparrow}{vx^*}\sqrt{\frac{(|v|-1)^2}{2\sqrt{2}(|v|+1)^2}\frac{|v|}{|u|}}\sqrt{\Theta_\downarrow}e^{-i\frac{(-\gamma+\phi_u+\delta_\downarrow)}{2}},$$

$$b_{3,d,\downarrow} = -\frac{u_\downarrow}{vx^*}\sqrt{\frac{(|v|-1)^2}{2\sqrt{2}(|v|+1)^2}\frac{|v|}{|u|}}\sqrt{\Theta_\uparrow}e^{-i\frac{(\gamma+\phi_u+\delta_\uparrow)}{2}},$$

$$b_{4,d,\downarrow} = -\frac{u_\downarrow}{v}\frac{\sqrt{2}}{|(|v|-1)|}\sqrt{\frac{(|v|-1)^2}{2\sqrt{2}(|v|+1)^2}\frac{|v|}{|u|}}\sqrt{\Theta_\downarrow}e^{-i\frac{(\phi_u+\delta_\downarrow)}{2}},$$

$$b_{4,d,\uparrow} = -\frac{u_\uparrow}{v}\frac{\sqrt{2}}{||v|-1|}\sqrt{\frac{(|v|-1)^2}{2\sqrt{2}(|v|+1)^2}\frac{|v|}{|u|}}\sqrt{\Theta_\uparrow}e^{-i\frac{(\phi_u+\delta_\uparrow)}{2}}.$$

$$a_{1,f,\uparrow} = -\frac{1}{x}\sqrt{\frac{(|v|-1)^2}{2\sqrt{2}(|v|+1)^2}\frac{|v|}{|u|}}\sqrt{\Theta_\uparrow}e^{i(\gamma+\phi_u+\delta_\uparrow)/2},$$

$$a_{1,f,\downarrow} = -\frac{1}{x}\sqrt{\frac{(|v|-1)^2}{2\sqrt{2}(|v|+1)^2}\frac{|v|}{|u|}}\sqrt{\Theta_\downarrow}e^{i(-\gamma+\phi_u+\delta_\downarrow)/2},$$

$$a_{2,f,\uparrow} = -\frac{\sqrt{2}}{|(|v|-1)|}\sqrt{\frac{(|v|-1)^2}{2\sqrt{2}(|v|+1)^2}\frac{|v|}{|u|}}\sqrt{\Theta_\downarrow}e^{i(\phi_u+\delta_\downarrow)/2},$$

$$a_{2,f,\downarrow} = -\frac{\sqrt{2}}{|(|v|-1)|}\sqrt{\frac{(|v|-1)^2}{2\sqrt{2}(|v|+1)^2}\frac{|v|}{|u|}}\sqrt{\Theta_\uparrow}e^{i(\phi_u+\delta_\uparrow)/2},$$

$$a_{3,f,\uparrow} = -\sqrt{\frac{(|v|-1)^2}{2\sqrt{2}(|v|+1)^2}\frac{|v|}{|u|}}\sqrt{\Theta_\uparrow}e^{i\frac{(\gamma+\phi_u+\delta_\uparrow+2\phi)}{2}},$$

$$a_{3,f,\downarrow} = \sqrt{\frac{(|v|-1)^2}{2\sqrt{2}(|v|+1)^2}\frac{|v|}{|u|}}\sqrt{\Theta_\downarrow}e^{i\frac{(-\gamma+\phi_u+\delta_\downarrow+2\phi)}{2}},$$

$$a_{4,f,\uparrow} = -\frac{v\sqrt{2}}{|(|v|-1)|}\sqrt{\frac{(|v|-1)^2}{2\sqrt{2}(|v|+1)^2}\frac{|v|}{|u|}}\sqrt{\Theta_\uparrow}e^{i\frac{(\phi_u+\delta_\uparrow+2\phi)}{2}},$$

$$a_{4,f,\downarrow} = \frac{v\sqrt{2}}{||v|-1|}\sqrt{\frac{(|v|-1)^2}{2\sqrt{2}(|v|+1)^2}\frac{|v|}{|u|}}\sqrt{\Theta_\downarrow}e^{i\frac{(\phi_u+\delta_\downarrow+2\phi)}{2}},$$

$$a_{1,d,\uparrow} = -\frac{u_\uparrow}{xv}\sqrt{\frac{(|v|-1)^2}{2\sqrt{2}(|v|+1)^2}\frac{|v|}{|u|}}\sqrt{\Theta_\downarrow}e^{-i\frac{(-\gamma+\phi_u+\delta_\downarrow+2\phi)}{2}},$$

$$a_{1,d,\downarrow} = \frac{u_\downarrow}{xv}\sqrt{\frac{(|v|-1)^2}{2\sqrt{2}(|v|+1)^2}\frac{|v|}{|u|}}\sqrt{\Theta_\uparrow}e^{-i\frac{(\gamma+\phi_u+\delta_\uparrow+2\phi)}{2}},$$

$$a_{2,d,\uparrow} = -\frac{u_\uparrow}{v^2}\frac{v^*\sqrt{2}}{||v|-1|}\sqrt{\frac{(|v|-1)^2}{2\sqrt{2}(|v|+1)^2}\frac{|v|}{|u|}}\sqrt{\Theta_\downarrow}e^{-i\frac{(\phi_u+\delta_\downarrow+2\phi)}{2}},$$

$$a_{2,d,\downarrow} = \frac{u_\downarrow}{v^2}\frac{v^*\sqrt{2}}{|(|v|-1)|}\sqrt{\frac{(|v|-1)^2}{2\sqrt{2}(|v|+1)^2}\frac{|v|}{|u|}}\sqrt{\Theta_\uparrow}e^{-i\frac{(\phi_u+\delta_\uparrow+2\phi)}{2}},$$

$$a_{3,d,\uparrow} = -\frac{u_\uparrow}{v}\sqrt{\frac{(|v|-1)^2}{2\sqrt{2}(|v|+1)^2}\frac{|v|}{|u|}}\sqrt{\Theta_\downarrow}e^{-i\frac{(-\gamma+\phi_u+\delta_\downarrow)}{2}},$$

$$a_{3,d,\downarrow} = -\frac{u_\downarrow}{v}\sqrt{\frac{(|v|-1)^2}{2\sqrt{2}(|v|+1)^2}\frac{|v|}{|u|}}\sqrt{\Theta_\uparrow}e^{-i\frac{(\gamma+\phi_u+\delta_\uparrow)}{2}},$$

$$a_{4,d,\downarrow} = -\frac{u_\downarrow}{v}\frac{v^*\sqrt{2}}{|(|v|-1)|}\sqrt{\frac{(|v|-1)^2}{2\sqrt{2}(|v|+1)^2}\frac{|v|}{|u|}}\sqrt{\Theta_\downarrow}e^{-i\frac{(\phi_u+\delta_\downarrow)}{2}},$$

$$a_{4,d,\uparrow} = -\frac{u_\uparrow}{v}\frac{v^*\sqrt{2}}{\big||v|-1\big|}\sqrt{\frac{(|v|-1)^2}{2\sqrt{2}(|v|+1)^2}\frac{|v|}{|u|}}\sqrt{\Theta_\uparrow}e^{-i\frac{(\phi_u+\delta_\uparrow)}{2}}.$$

Here $\gamma, u_\sigma, \sigma = \uparrow, \downarrow$ are arbitrary ($\neq 0, \infty$) numerical parameters, $v = |v|e^{i\phi_u}$, $x = |x|e^{i\phi_u}$ and $|x| = \frac{|v|-1}{|v|+1}$. The $\frac{|v|}{|u|}$ ratio and the $\delta_\uparrow - \delta_\downarrow$ phase (with the choise $\chi = \phi_u + \phi = \frac{\pi}{2}$) can be expressed as

$$\frac{|v|}{|u|} = \frac{-t_x^f}{\sqrt{\Theta_\uparrow\Theta_\downarrow}\cos\frac{\delta_\uparrow-\delta_\downarrow}{2}}, \qquad \tan\frac{\delta_\uparrow-\delta_\downarrow}{2} = \frac{t_y^f}{t_x^f}.$$

A
lso η is obtainable via ε_f

$$\eta = \varepsilon_f + U_f - 4\frac{1+|v|^2}{(|v|-1)^2}\left(\left|b_{1,f,\uparrow}\right|^2 + \left|b_{1,f,\downarrow}\right|^2\right).$$

REFERENCES

[1] Spavieri, G., Mansuripur, M. (2015). Origin of the spin–orbit interaction. *Physica Scripta*, vol. 90, no. 8, p. 085501, June 2015 [online]. Available: https://iopscience.iop.org/article/10.1088/0031-8949/90/8/085501/meta

[2] Baym, G. (1973). *Lectures on quantum mechanics*. Chapter 23, Benjamin-Cummings Publishing Co.

[3] Bychkov, Y. A., Rashba, E. I. (1984). Properties of a 2D Electron Gas with Lifted Spectral Degeneracy. *JETP Letters*, vol. 39, no. 2, pp. 78–83 [online]. Available: http://www.jetpletters.ac.ru/ps/1264/article_19121.shtml

[4] Dresselhaus, G. (1955). Spin-Orbit Coupling Effects in Zinc Blende Structures. *Phys. Rev.*, vol. 100, no. 2, pp. 580–586, October 1955 [online]. Available: https://link.aps.org/doi/10.1103/PhysRev.100.580.

[5] Li, Z., Covaci, L., Marsiglio, F. (2012). Impact of Dresselhaus versus Rashba spin-orbit coupling on the Holstein polaron. *Phys. Rev. B.*, vol. 85, no. 20, p. 205112, May 2012 [online]. Available: https://link.aps.org/doi/10.1103/PhysRevB.85.205112.

[6] Kosterlitz, J. M., Thouless, D. J. (1973). Ordering, metastability and phase transitions in two-dimensional systems. *Journal of Physics C: Solid State Physics*, vol. 6, no. 7, p. 1181 [online]. Available: https://doi.org/10.1088/0022-3719/6/7/010.

[7] Huang, J., Pfeiffer, L. N., West, K. W. (2017). Spin-orbit coupling and transport in strongly correlated two-dimensional systems. *Phys. Rev. B*, vol. 95, no. 19, p. 195139, May 2017 [online]. Available: https://link.aps.org/doi/10.1103/PhysRevB.95.195139.

[8] Shaffer, R., Lee, E. K. H., Yang, B. J., Kim, Y. B. (2016). Recent progress on correlated electron systems with strong spin–orbit coupling. *Reports on Progress in Physics*, vol. 79, no 9, p. 094504, August 2016 [online]. Available: https://doi.org/10.1088/0034-4885/79/9/094504.

[9] Brinkman, A., Huiben, M., van Zalk, M. et al. (2007). Magnetic effects at the interface between non-magnetic oxides. *Nat. Matter*, vol. 6, p. 493, June 2007 [online]. Available: https://www.nature.com/articles/nmat1931.

[10] Raman, K. V., Moodera, J. S. (2015). A magnetic facelift for non-magnetic metals. *Nature*, vol. 524, p. 42, August 2015 [online]. Available: https://www.nature.com/articles/524042a.

[11] Raul, J. G., Lee, E. K. H., Kee, H. Y. (2015). Spin-Orbit Physics Giving Rise to Novel Phases in Correlated Systems: Iridates and Related Materials. *Annual Review of Condensed Matter Physics*, vol. 7, p. 195, December 2015 [online]. Available: https://doi.org/10.1146/annurev-conmatphys-031115-011319.

[12] Gangopadhyay, S., Pickett, W. E. (2016). Spin-orbit coupling, strong correlation, and insulator-metal transitions: The $J_{eff} = \frac{3}{2}$ ferromagnetic Dirac-Mott insulator $Ba_2\ NaOsO_6$. *Phys. Rev. B*, vol. 93, no. 4, p. 155126, January 2016 [online]. Available: https://link.aps.org/doi/10.1103/PhysRevB.91.045133

[13] Gulácsi, Z. (2013). Exact ground states of correlated electrons on pentagon chains. *International Journal of Modern Physics B*, vol. 27, no. 14, p. 1330009, May 2013 [online]. Available: http://doi.org/10.1142/S0217979213300090.

[14] Gulácsi, Z., Vollhardt, D. (2003). Exact Insulating and Conducting Ground States of a Periodic Anderson Model in Three Dimensions. *Phys. Rev. Lett.*, vol. 91, no. 18, p. 186401, October 2003 [online]. Available: http://link.aps.org/doi/10.1103/PhysRevLett.91.186401.

[15] Gulácsi, Z., Kampf, A., Vollhardt, D. (2007). Exact Many-Electron Ground States on the Diamond Hubbard Chain. *Phys. Rev. Lett.*, vol. 99, no. 2, p. 026404, July 2007 [online]. Available: http://link.aps.org/doi/10.1103/PhysRevLett.99.026404.

[16] Gulácsi, Z., Kampf, A., Vollhardt, D. (2010). Route to Ferromagnetism in Organic Polymers. *Phys. Rev. Lett.*, vol. 105, no. 26, p. 266403, December 2010 [online]. Available: http://link.aps.org/doi/10.1103/PhysRevLett.105.266403.

[17] Gulácsi, Z., Vollhardt, D. (2005). Exact ground states of the periodic Anderson model in D = 3 dimensions. *Phys. Rev. B*, vol. 72, no. 7, p. 075130, August 2005 [online]. Available: http://link.aps.org/doi/10.1103/PhysRevB.72.075130.

[18] Gulácsi, Z. (2004). Exact multielectronic electron-concentration-dependent ground states for disordered two-dimensional two-band systems in the presence of disordered hoppings and finite on-site random interactions. *Phys. Rev. B*, vol. 69, no. 5, p. 054204, February 2004 [online]. Available: http://link.aps.org/doi/10.1103/PhysRevB.69.054204.

[19] Gulácsi, Z., Gulácsi, M. (2006). Exact stripe, checkerboard, and droplet ground states in two dimensions. *Phys. Rev. B*, vol. 73, no. 1, p. 014524, January 2006 [online]. Available: http://link.aps.org/doi/10.1103/PhysRevB.73.014524.

[20] Kollar, M., Strack, R., Vollhardt, D. (1996). Ferromagnetism in correlated electron systems: Generalization of Nagaoka's theorem. *Phys. Rev. B*, vol. 53, no. 14, p. 9225, April 1996 [online]. Available: http://link.aps.org/doi/10.1103/PhysRevB.53.9225.